nature chemical biology

SUPPLEMENTARY INFORMATION

https://doi.org/10.1038/s41589-019-0402-7

In the format provided by the authors and unedited.

Engineering a nicotinamide mononucleotide redox cofactor system for biocatalysis

William B. Black[1,6], Linyue Zhang[1,6], Wai Shun Mak[2,3,6], Sarah Maxel[1], Youtian Cui[2,3], Edward King[4], Bonnie Fong[1], Alicia Sanchez Martinez[1], Justin B. Siegel[2,3,5]* and Han Li[1]*

[1]Department of Chemical and Biomolecular Engineering, University of California, Irvine, Irvine, CA, USA. [2]Department of Chemistry, University of California, Davis, Davis, CA, USA. [3]Genome Center, University of California, Davis, Davis, CA, USA. [4]Department of Molecular Biology and Biochemistry, University of California, Irvine, Irvine, CA, USA. [5]Department of Biochemistry and Molecular Medicine, University of California, Davis, Davis, CA, USA. [6]These authors contributed equally: William B. Black, Linyue Zhang, Wai Shun Mak. *e-mail: jbsiegel@ucdavis.edu; han.li@uci.edu

Engineering a nicotinamide mononucleotide redox cofactor system for biocatalysis

William B. Black[1,6],Linyue Zhang[1,6],Wai Shun Mak[2,3,6], Sarah Maxel[1], Youtian Cui[2,3], Edward King[4], Bonnie Fong[1], Alicia Sanchez Martinez[1] , Justin B. Siegel[2,3,5,*], and Han Li[1,*]

[1]Department of Chemical and Biomolecular Engineering, University of California, Irvine, Irvine, CA, [2]Department of Chemistry, University of California, Davis, Davis, CA,[3]Genome Center, University of California, Davis, Davis, CA, [4]Department of Molecular Biology and Biochemistry, University of California, Irvine, Irvine, CA,[5]Department of Biochemistry and Molecular Medicine, University of California, Davis, Davis, CA.
*[6]These authors contributed equally to this work. *To whom correspondence should be addressed. Email: han.li@uci.edu, jbsiegel@ucdavis.edu*

Supplementary information

Supplementary Table 1: Sequence conservation analysis of I195 in its protein family PF13561.5.

	Frequency	Percent of representation
A	110	2.50%
C	2	0.00%
D	33	0.70%
E	31	0.70%
F	461	10.40%
G	112	2.50%
H	10	0.20%
I	371	8.40%
K	20	0.50%
L	899	20.30%
M	1,768	39.90%
N	42	0.90%
P	21	0.50%
Q	97	2.20%
R	65	1.50%
S	67	1.50%
T	210	4.70%
V	45	1.00%
W	52	1.20%
Y	15	0.30%

This result showed that all 20 amino acids are represented at this position with methionine and leucine accounting for more than 50% of all occurrences at this position in the family.

Supplementary Table 2: Full Steady-State Kinetics Parameters

Enzyme	Cofactor	K_{ia} (mM)	k_{cat} (s^{-1})	K_A (mM)	K_B (mM)	k_1 ($mM^{-1}s^{-1}$)	k_2 (s^{-1})	k_3 ($mM^{-1}s^{-1}$)	(k_1k_3/k_2) ($mM^{-2}s^{-1}$)
Bs GDH WT	NAD^+	$(6.8\pm2.0) \times 10^{-2}$	$(3.7\pm0.5) \times 10^{1}$	$(5.1\pm0.2) \times 10^{-2}$	8.3±2.8	$(7.2\pm1.3) \times 10^{2}$	$(5.0\pm2.3) \times 10^{1}$	4.8±2.3	$(6.9\pm1.3) \times 10^{1}$
	$NADP^+$	$(8.5\pm0.4) \times 10^{-3}$	$(3.0\pm0.7) \times 10^{1}$	$(1.0\pm0.1) \times 10^{-2}$	7.2±0.8	$(3.0\pm0.4) \times 10^{3}$	$(2.5\pm0.2) \times 10^{1}$	4.1±0.6	$(4.9\pm0.9) \times 10^{2}$
	NMN^+	n.d.[a]	n.d.[a]	n.d.[a]	n.d.[a]	$(8.6\pm2.2) \times 10^{-2}$	n.d.[a]	n.d.[a]	$(2.5\pm0.3) \times 10^{-4}$
Bs GDH Triple (I195R-A93K-Y39Q)	NAD^+	n.d.[b]	n.d.[b]	n.d.[b]	n.d.[b]	n.d.[b]	n.d.[b]	$(2.6\pm0.2) \times 10^{-4}$	$(6.6\pm1.1) \times 10^{-5}$
	$NADP^+$	4.6±0.6	$(3.7\pm1.3) \times 10^{-1}$	$(4.7\pm2.3) \times 10^{1}$	$(1.7\pm0.6) \times 10^{2}$	$(8.8\pm3.0) \times 10^{-2}$	$(4.2\pm1.8) \times 10^{-1}$	$(2.2\pm0.1) \times 10^{-3}$	$(4.8\pm0.6) \times 10^{-4}$
	NMN^+	$(3.4\pm0.6) \times 10^{-1}$	$(4.1\pm0.1) \times 10^{-1}$	$(1.9\pm0.2) \times 10^{-1}$	$(9.0\pm1.6) \times 10^{1}$	$(2.2\pm0.2) \times 10^{1}$	$(7.5\pm1.8) \times 10^{-1}$	$(4.7\pm0.8) \times 10^{-3}$	$(1.4\pm0.1) \times 10^{-2}$
Bs GDH Ortho (I195R-A93K-Y39Q-S17E)	NAD^+	n.d.[a]	n.d.[a]	n.d.[a]	n.d.[a]	$(1.4\pm0.7) \times 10^{-3}$	n.d.[a]	n.d.[a]	$(0.6\pm0.2) \times 10^{-5}$
	$NADP^+$	$(5.2\pm0.5) \times 10^{-1}$	$(2.9\pm0.3) \times 10^{-1}$	$(6.5\pm1.4) \times 10^{-1}$	$(4.2\pm0.7) \times 10^{2}$	$(4.6\pm1.0) \times 10^{-1}$	$(2.4\pm0.3) \times 10^{-1}$	$(7.1\pm0.9) \times 10^{-4}$	$(1.4\pm0.1) \times 10^{-3}$
	NMN^+	4.6±2.7	$(2.7\pm0.7) \times 10^{-1}$	4.9±4.1	$(3.9\pm1.2) \times 10^{1}$	$(8.9\pm6.4) \times 10^{-2}$	$(3.1\pm2.2) \times 10^{-1}$	$(6.8\pm0.3) \times 10^{-3}$	$(2.4\pm2.1) \times 10^{-3}$

Reactions were performed in 35 mM Tris-HCl buffer (pH 8.0) at 25 °C. k_{cat} is turnover number, K_A and K_B are full steady-state Michaelis constants for cofactor and substrate, respectively. k_{ia} is the dissociation constant for cofactor binding. k_1 is the on-rate of cofactor, k_2 is the off-rate of cofactor, k_3 is the on-rate of glucose. The microscopic reaction rates were calculated from the relationships $k_1 = k_{cat}/K_A$, $k_2 = k_{cat}\ k_{ia}\ /K_A$, $k_3 = k_{cat}/K_B$. Detailed rate equations can be found in Methods. Errors shown are the standard deviation of three independent measurements.

[a]Not determined. Enzyme could not be saturated with cofactor concentrations tested.

[b]Not determined. Enzyme could not be saturated with glucose concentrations tested.

Supplementary Table 3: Plasmids and strains used in this study

Strains	**Description**	**Reference**
XL-1 Blue	Cloning strain	Stratagene
BL21 (DE3)	Protein expression strain	Invitrogen
BW25113	*E. coli* Δ(*araD-araB)567*, Δ*lacZ4787(*::rrnB-3), *λ*-, *rph*-1, Δ*(rhaD-rhaB)568*, *hsdR514*	Keio Collection
JW2670-1	BW25113 Δ*pncC::kan*	Keio Collection
MX101	BW25113 Δ*pncC* Δ*nadR::kan*	This study
MX102	BW25113 Δ*pncC* Δ*pgi* Δ*zwf* Δ*gntK::kan*	This study
MX103	BW25113 Δ*pncC* Δ*pgi* Δ*zwf* Δ*nadR* Δ*gnd::kan*	This study
Plasmids	**Description**	**Reference**
pEK101	P_{LlacO1}*::Bs gdh*, ColE1 *ori*, Amp^R	This study
pEK102	P_{LlacO1}*::Pp xenA*, ColE1 *ori*, Amp^R	This study
pLZ201	P_{LlacO1}*::Bs gdh* N92A, ColE1 *ori,* Amp^R	This study
pLZ202	P_{LlacO1}*::Bs gdh* N92V, ColE1 *ori,* Amp^R	This study
pLZ203	P_{LlacO1}*::Bs gdh* G94S, ColE1 *ori*, Amp^R	This study
pLZ204	P_{LlacO1}*::Bs gdh* I195R, ColE1 *ori*, Amp^R	This study
pLZ205	P_{LlacO1}*::Bs gdh* I195S, ColE1 *ori*, Amp^R	This study
pLZ206	P_{LlacO1}*::Bs gdh* I195T, ColE1 *ori*, Amp^R	This study
pLZ207	P_{LlacO1}*::Bs gdh* S17Q-P194N, ColE1 *ori*, Amp^R	This study
pLZ208	P_{LlacO1}*::Bs gdh* M143S, ColE1 *ori,* Amp^R	This study
pLZ209	P_{LlacO1}*::Bs gdh* M143T, ColE1 *ori*, Amp^R	This study
pLZ210	P_{LlacO1}*::Bs gdh* I195R-A93K-Y39Q, ColE1 *ori*, Amp^R	This study
pLZ211	P_{LlacO1}*::Bs gdh* I195R-Y39Q, ColE1 *ori*, Amp^R	This study
pLZ212	P_{LlacO1}*::Bs gdh* I195R-A93K, ColE1 *ori*, Amp^R	This study
pLZ213	P_{LlacO1}*::Bs gdh* A93K, ColE1 *ori*, Amp^R	This study
pLZ214	P_{LlacO1}*::Bs gdh* Y39Q, ColE1 *ori*, Amp^R	This study
pLZ215	P_{LlacO1}*::Bs gdh* A93K-Y39Q, ColE1 *ori*, Amp^R	This study
pLZ216	P_{LlacO1}*::Bs gdh* I195R-A93K-Y39Q-S17E, ColE1 *ori*, Amp^R	This study
pLZ217	P_{BAD}*::Pp xenA*, RSF *ori*, $Spec^R$	This study
pLZ218	P_{BAD}*::Bs gdh* I195R-A93K-Y39Q-S17E - *Pp xenA*, RSF *ori*, $Spec^R$	This study

pLZ219	P_{BAD}::*Bs gdh* - *Pp xenA*, RSF *ori*, $Spec^R$	This study
pLZ220	P_{BAD}::*Bs gdh* - *Ca lvr*, RSF *ori*, $Spec^R$	This study
pLZ221	P_{BAD}::*Bs gdh* I195R-A93K-Y39Q-S17E - *Ca lvr*, RSF *ori*, $Spec^R$	This study
pLZ222	P_{BAD}::*Ca lvr*, RSF *ori,* $Spec^R$	This study
pLZ223	P_{BAD}::*Bs gdh* - *Rs adh*, RSF *ori*, $Spec^R$	This study
pLZ224	P_{BAD}::*Bs gdh* I195R-A93K-Y39Q-S17E - *Rs adh*, RSF *ori*, $Spec^R$	This study
pLZ225	P_{BAD}::*Rs adh*, RSF *ori*, $Spec^R$	This study
pLZ226	P_{LlacO1}::*Pp xenA* - *Ca lvr* - *Rs adh*, ColE1 *ori*, Amp^R	This study
pSM101	P_{LlacO1}::*Bm BM3*, ColE1 *ori*, Amp^R	This study
pSM102	P_{LlacO1}::*Bm BM3* W1046S, ColE1 *ori*, Amp^R	This study
pSM103	P_{LlacO1}::*Ft nadEV* - *Zm glf* - *Re gntK*, ColE1 *ori*, Amp^R	This study
pSM104	P_{LlacO1}::*Zm glf*, ColE1 *ori*, Amp^R	This study
pSM105	P_{LlacO1}::*Empty*, ColE1 *ori*, Amp^R	This study
pSM106	P_{BAD}::*Bs gdh* I195R-A93K-Y39Q-S17E, RSF *ori*, $Spec^R$	This study
pSM107	P_{BAD}::*Bs gdh*, RSF *ori*, $Spec^R$	This study
pSM108	P_{BAD}::*Empty*, RSF *ori*, $Spec^R$	This study
pSM109	P_{LlacO1}::*Zm glf*, p15A *ori*, Cm^R	This study
pSM110	P_{LlacO1}::*Zm glf*, ColE1 *ori*, Cm^R	This study
pWB201	P_{LlacO1}::*Sc OYE3*, ColE1 *ori*, Amp^R	This study
pWB202	P_{LlacO1}::*Ec nfsB*, ColE1 *ori*, Amp^R	This study
pWB203	P_{LlacO1}::*Ft nadEV*, ColE1 *ori*, Amp^R	This study

Abbreviations indicate source of genes: *Ca*, *Corynebacterium aquaticum*; *Bm, Bacillus megaterium*; *Bs*, *Bacillus subtilis*; *Ft*, *Francisella tularensis*; *Pp*, *Pseudomonas putida*; *Re*, *Ralstonia eutropha H16*; *Rs*, *Ralstonia sp.*; *Sc*, *Saccharomyces cerevisiae*; *Zm*, *Zymomonas mobilis*

Supplementary Table 4: Accession numbers for proteins used in this study

Protein Name	Full Name	Protein ID
Ec PncC	NMN aminohydrolase	P0A6G3.1
Ec NadR	NMN adenylyltransferase	P27278.2
Ec Pgi	Glucose-6-phosphate isomerase	P0A6T1
Ec Zwf	NADP(+)-dependent glucose-6-phosphate dehydrogenase	P0AC53
Ec Gnd	6-phosphogluconate dehydrogenase	P00350
Ec GntK	D-gluconate kinase	P46859
Ec NfsB	Oxygen-insensitive NAD(P)H nitroreductase	P38489
Ft NadE	NAD(+) synthase	Q5NFH5
Ft NadV	Nicotinate phosphoribosyltransferase	A0A4Q7HER8
Zm Glf	Glucose facilitated diffusion porin	A0A2R4S350
Sc OYE3	Old Yellow Enzyme 3	P41816
Re GntK	D-Gluconate kinase	Q0KCF1
Bm BM3	Bifunctional fatty acid monooxygenase	Addgene plasmid #85102
Bs Gdh	Glucose 1-dehydrogenase	P12310
Pp XenA	NADH: flavin oxidoreductase/NADH oxidase	Q9R9V9
Ca LVR	Levodione reductase	Q9LBG2.1
Rs ADH	Alcohol dehydrogenase	ACB78191.1

Supplementary Table 5 Mass spectrometry parameters for Intracellular cofactor concentration analysis

Compound	Primary Mass	Secondary Mass	Cone Voltage	Collison Energy
MNA^+ (IS)	137	94	20	20
NMN^+	335	123	10	10
NAD^+	664	135.9	20	40

IS: internal standard

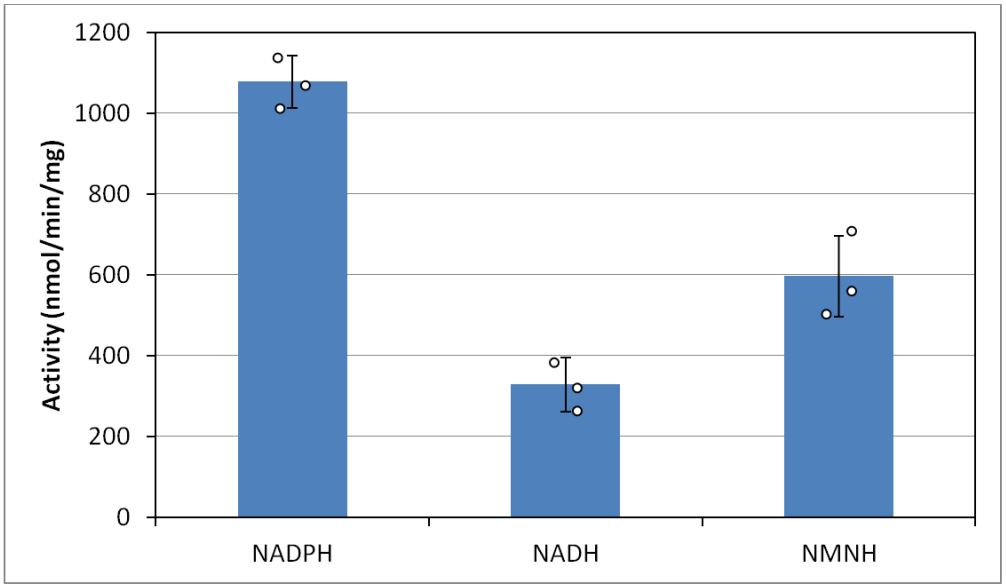

Supplementary Figure 1: XenA activity with different cofactors. Using ketoisophorone as the substrate, the activity of purified *Pseudomonas putida* XenA wild type was tested, using NADPH, NADH, or NMNH as the reducing cofactor. The error bars represent the standard deviations of three replicates. These results showed that XenA accepts NMNH as the redox cofactor with comparable activity to the natural cofactors NADPH and NADH. Detailed enzyme assay condition is described in the Methods section.

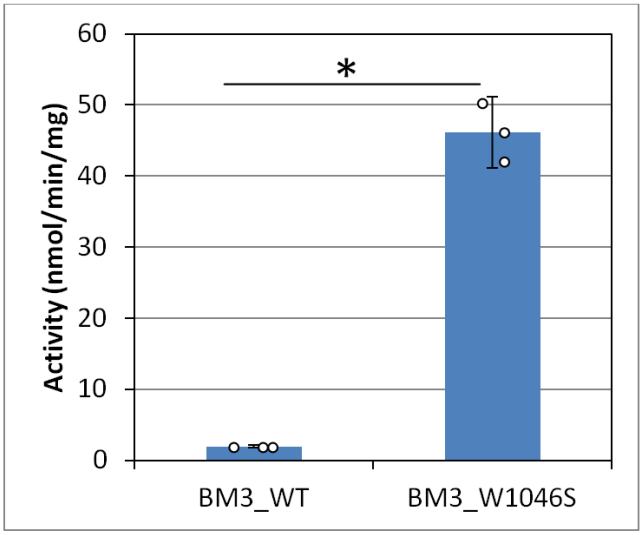

Supplementary Figure 2: Engineering P450 BM3 to improve the NMNH-dependent activity. Using cytochrome *c* as the substrate, the NMNH-dependent activity of P450 BM3 wild type and W1046S was measured using purified proteins. The error bars represent the standard deviations of three replicates. The results showed that the W1046S mutation enhanced the NMNH-dependent activity by around 46-fold compared to the wild type. Values are an average of at least three replicates with error bars representing one standard deviation. Two-tailed t-tests were used to determine statistical significance ($P < 0.05$), indicated by an asterisk. Detailed enzyme assay condition is described in the Methods section.

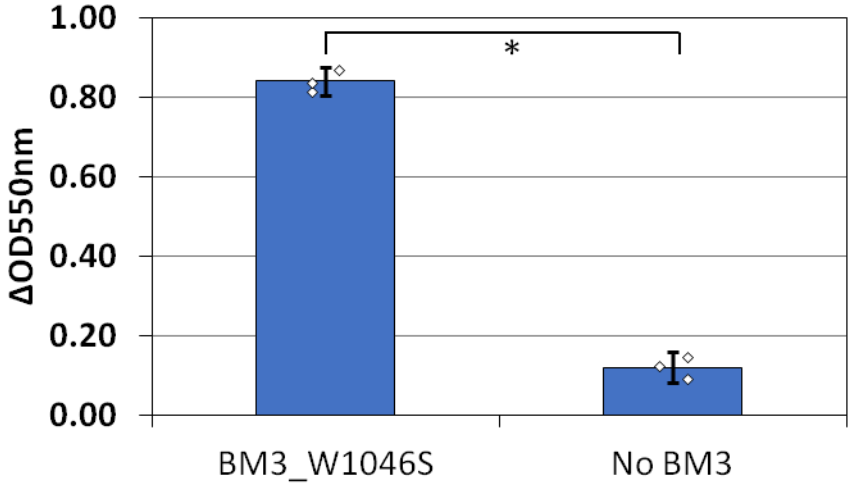

Supplementary Figure 3: Cytochrome *c* reduction in the presence and absence of P450 enzyme

Engineering P450 BM3-W1046S facilitated cytochrome *c* reduction via NMN^+ cycling by Bs GDH Triple. The results showed that without BM3 W1046S, the reduction of cytochrome *c*, as indicated by the change of absorbance at 550nm (ΔOD550nm), was minimal compared to in the presence of the enzyme. Values are an average of at least three replicates with error bars represent one standard deviation. Two-tailed t-tests were used to determine statistical significance ($P < 0.05$), indicated by an asterisk.

Coupled enzymatic biotransformation condition was used as described in the Methods section. BM3 was added at a concentration of 0.34 mg mL^{-1} and 50 μM cytochrome *c* (C2506, Sigma) was used as the substrate.

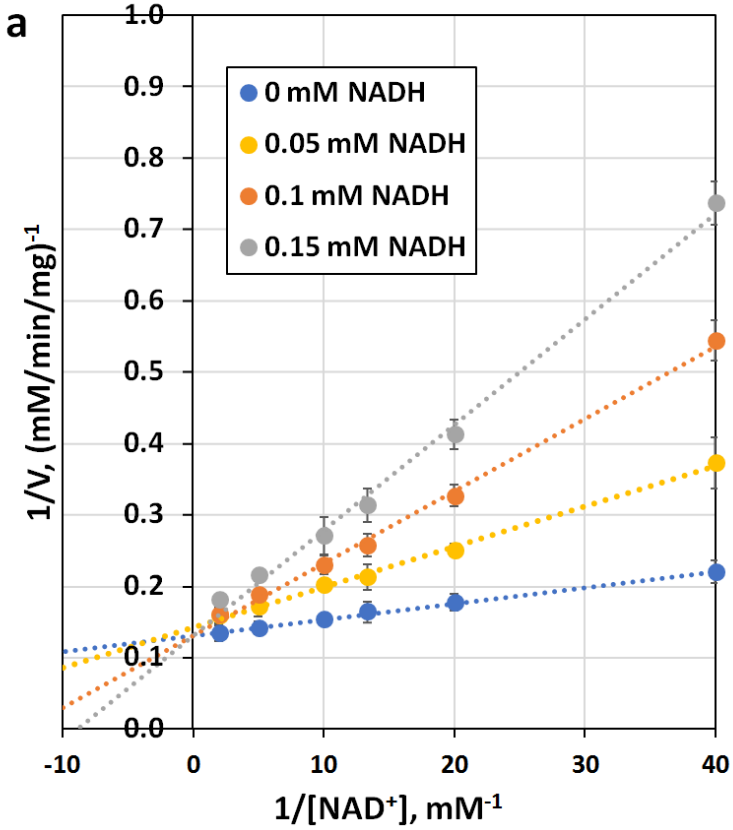
a
0 mM NADH
0.05 mM NADH
0.1 mM NADH
0.15 mM NADH
1/V, (mM/min/mg)-1
1/[NAD+], mM-1
1.0
0.9
0.8
0.7
0.6
0.5
0.4
0.3
0.2
0.1
0.0
-10
0
10
20
30
40

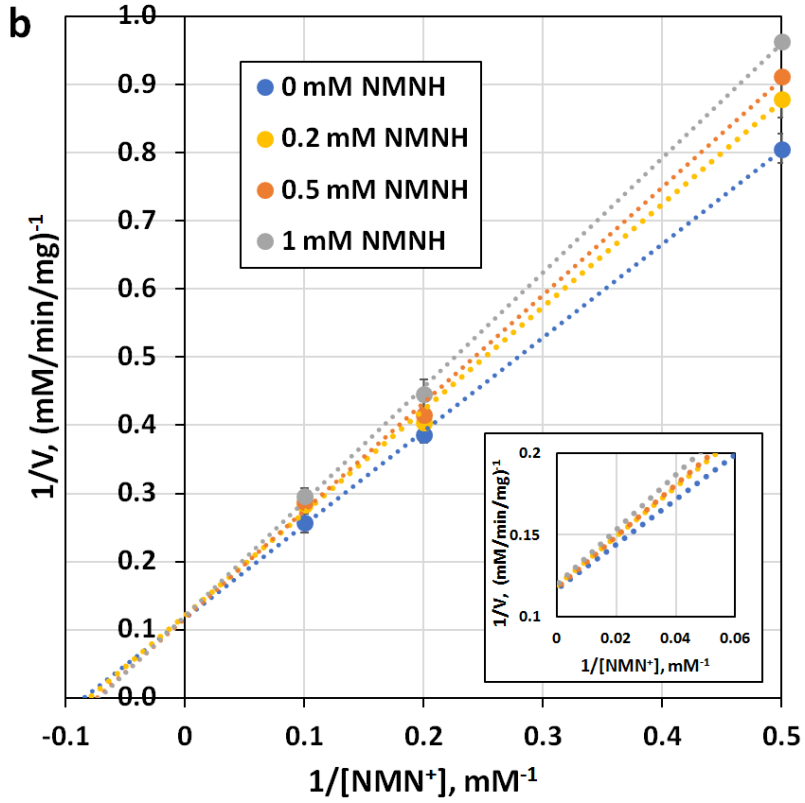
b
0 mM NMNH
0.2 mM NMNH
0.5 mM NMNH
1 mM NMNH
1/V, (mM/min/mg)-1
1/[NMN+], mM-1
1.0
0.9
0.8
0.7
0.6
0.5
0.4
0.3
0.2
0.1
0.0
-0.1
0
0.1
0.2
0.3
0.4
0.5
0.2
0.15
0.1
0
0.02
0.04
0.06

Supplementary Figure 4: Production inhibition study of wild type and engineered Bs GDH

(a) Product inhibition of wild type GDH by NADH. NAD^+ was varied from 0.5 to 0.025 mM. NADH was supplied at 0, 0.05, 0.1, or 0.15mM. (b) Product inhibition of Bs GDH Ortho (I195R-A93K-Y39Q-S17E) by NMNH. NMN^+ was varied from 2 to 10 mM. NMNH was supplied at 0, 0.2, 0.5, or 1 mM. Inset is a scale-in view of conversion at the y-axis. Glucose was held constant at 50mM for both (a) and (b). Error bars represent one standard deviation of the mean of triplicate experiments. See detailed enzyme assay method in the Methods section.

The results showed that NMNH is a competitive inhibitor for NMN^+ (b), indicating that the engineered Bs GDH Ortho catalyzes the NMN^+-dependent reaction with a ordered bi-bi mechanism. The same mechanism is used by wild type Bs GDH (a).

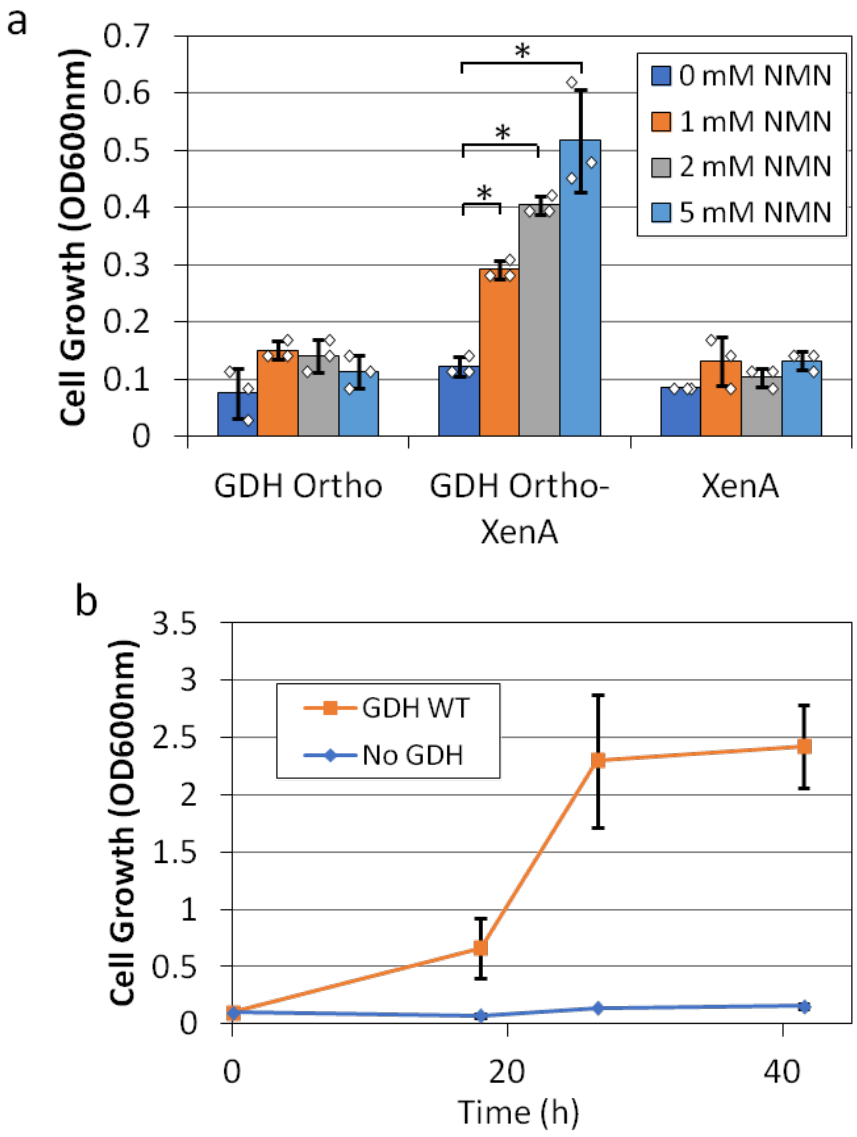

Supplementary Figure 5: Dependence of growth on NMN^+ concentration

a. Increased supplementation of NMN^+ supports faster growth via increased Bs GDH Ortho cycling with XenA (NMNH-redox cycling partner). In the strain used (Strain MX103), cell growth was directly tied to Bs GDH activity in minimal glucose media and cofactor regeneration via XenA activity. Metabolism of glucose was limited to the Entner–Doudoroff (ED) pathway in this strain (*Δpgi, Δzwf, Δgnd*). Therefore, entry to glycolysis for glucose was dependent on Bs GDH Ortho conversion of glucose to gluconate, which was then converted to gluconate-6-phosphate via *gntK*

(*Ralstonia eutropha gntK* was overexpressed to facilitate metabolism). Although native intracellular NMN^+ concentration had been increased in this strain via deletion of NMN^+ degrading pathways (*ΔpncC, ΔnadR*) and heterologous expression of NMN+ producing genes (*Francisella tularensis nadEV*), higher cell growth with higher NMN^+ supplement indicated increased metabolism of glucose via Bs GDH activity. The dependence of growth on NMN^+ concentration is only seen in cells that harbor both Bs GDH Ortho and XenA, but not in cells with either of the two redox partners omitted. The error bars represent one standard deviation above the mean of triplicate experiments. Two-tailed t-tests were used to determine statistical significance ($P < 0.05$), indicated by an asterisk.

b. Expression of Bs GDH WT enabled robust growth in the single glycolytic pathway (ED pathway) engineered strain MX103 in minimal glucose media. Native cell metabolism was able to supply Bs GDH WT (red) with $NAD(P)^+$ to support glucose to gluconate cycling without additional cofactor supplementation or a heterologous redox cycling partner. Without expression of Bs GDH (blue), this strain did not demonstrate glucose metabolism. The error bars represent one standard deviation above the mean of triplicate experiments.

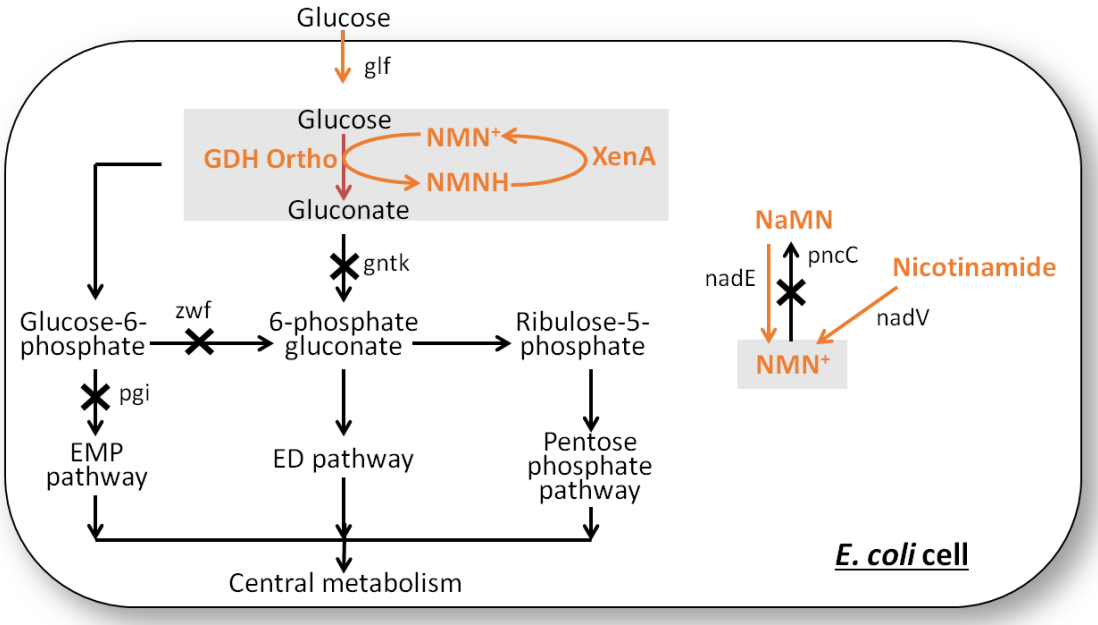

Supplementary Figure 6: **Strain engineered for whole-cell catalyst limits glucose consumption and cofactor regeneration to Bs GDH activity.** Disruption of main glycolytic pathways (*Δpgi, Δzwf , ΔgntK*) eliminated native glucose metabolism. These deletions limited cofactor reduction to only Bs GDH activity in whole cell conversion assays in phosphate buffer. Direct transport of glucose into the cell was enabled by expression of glucose facilitator (Glf). Disruption of NMN^+ degrading gene (*ΔpncC*) and overexpression of NMN^+ producing genes (*nadE, nadV*) enabled elevated intracellular levels of NMN^+ for Bs GDH Ortho cycling.

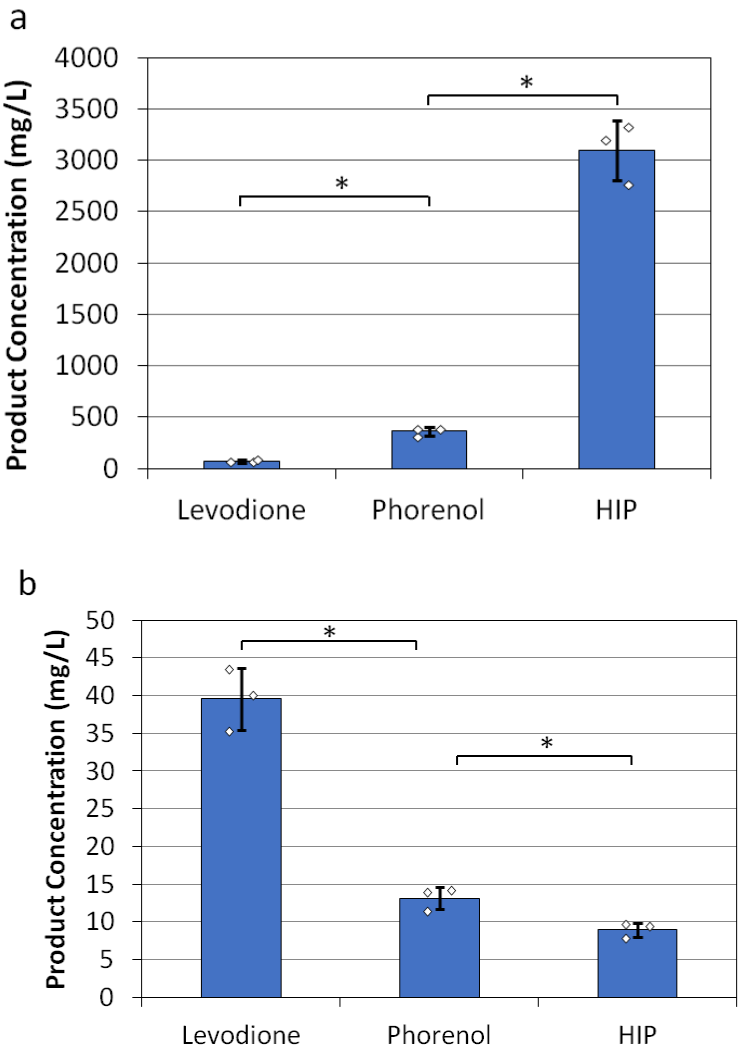

Supplementary Figure 7: **Product levels in whole-cell ketoisophorone (KIP) conversion with co-expression of XenA, LVR, and ADH.** With simultaneous expression of all three KIP converting enzymes, the principal product was determined by the cofactor specificity of GDH. (a) Production of 4-hydroxyisophorone (HIP) was dominant when the redox system was coupled with GDH WT ($NAD(P)^+$ preference). (b) Production of levodione was dominant when the redox system was coupled with GDH Ortho (NMN^+ preference). XenA, enoate reductase from *Pseudomonas putida*. LVR, levodione reductase from *Corynebacterium aquaticum*. ADH, alcohol dehydrogenase from *Ralstonia sp*. The error bars represent one standard deviation above the mean of triplicate experiments. Two-tailed t-tests were used to determine statistical significance ($P < 0.05$), indicated by an asterisk.

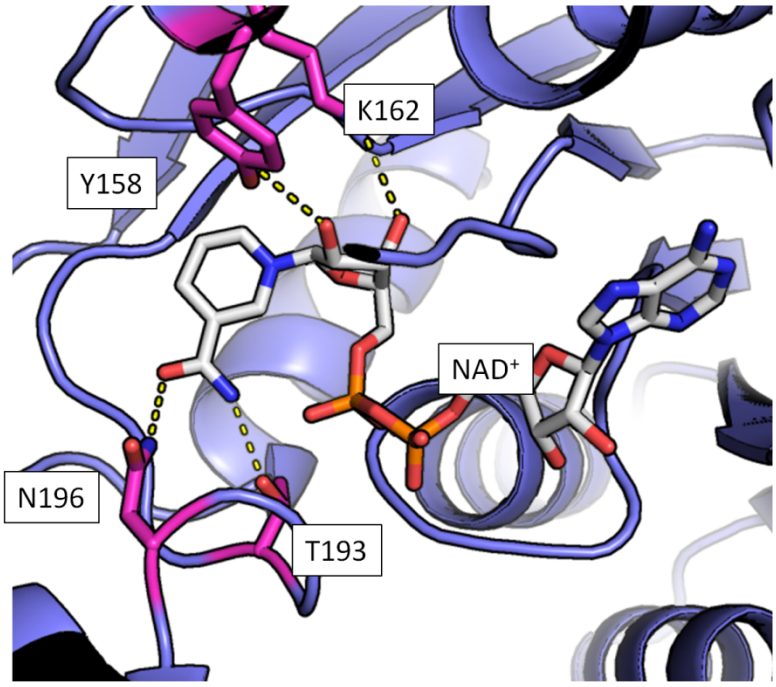

Supplementary Figure 8 Active site of glucose dehydrogenase with NAD^+ bound (PDB:1GCO).The catalytic residues Y158 and K162 participate in a hydrogen bond network with the hydroxyl groups on the ribose from the nicotinamide half of the NAD^+ molecule. The hydrogen bonds between both N196 and T193 to the amide on NAD^+ suggest that they are potentially critical to the orientation of NAD^+ into a catalytically relevant binding conformation primed for the hydride transfer step.